# Magnetosonic shock waves in magnetized quantum plasma with the evolution of spin-up and spin-down electrons

Zakia Rahim,[1] Muhammad Adnan,[2] and Anisa Qamar[1]
[1]*Department of Physics, University of Peshawar, Peshawar 25000, Pakistan*
[2]*Department of Physics, Kohat University of Science & Technology (KUST), Kohat, Pakistan*

(Received 13 May 2019; published 27 November 2019)

The quantum hydrodynamic model is used to study the linear and nonlinear properties of small amplitude magnetosonic shock waves in dissipative plasma with degenerate inertialess spin-up and spin-down electrons and inertial classical ions. Spin effects are considered via spin pressure and macroscopic spin magnetization current. A linear dispersion relation is derived analytically and plotted numerically for different plasma parameters such as spin density, polarization ratio, plasma beta, quantum diffraction, spin magnetization energy, and magnetic diffusivity. Employing the standard reductive perturbation technique, a Korteweg–de Vries–Burgers-type equation is derived for small amplitude waves and studied numerically. We have observed that an oscillatory and monotonic shock waves are generated depending upon the plasma configurations. The phase portraits of both oscillatory and monotonic shock waves are also presented. Interestingly, different plasma parameters are found to play a significant role in the transition of oscillatory to monotonic shock waves or vice versa. Most importantly it is found that, the magnetosonic excitations obtained with spin-up and spin-down electrons are significantly different from the usual electron ion quantum plasma. The work presented is related to magnetosonic waves in dense astrophysical environments such as a pulsar magnetosphere and neutron stars.

DOI: 10.1103/PhysRevE.100.053206

## I. INTRODUCTION

The two fundamental plasma configurational parameters, density and temperature, which characterize plasma can proliferate over several orders. For low density and high temperature situations, the collective modes and instabilities can be fully described by the classical Newtonian mechanics [1,2]. However, the form of plasmas found in many cases, for instance, in compact astrophysical objects [3], planetary interiors, the cores of giant planets [4,5], the crusts of cold stars, intense laser-solid density plasma experiments [6,7], miniaturized semiconducting devices [8], and quantum x-ray free-electron lasers, are extremely dense and can have temperature substantially lower than that of the classical plasma [9]. The energy contents in such plasmas (particles and/or fields) exceed the thermal energy contents. The de Broglie wavelength, $\lambda_D$, which is the spatial extent of the particle wavefunction, becomes comparable to the interparticle distance, making the wavefunctions of the adjacent particles overlap; i.e., $\lambda_D(=h/2\pi m v_t) \geqslant \sqrt{n-3}$ (where $n$ represents the equilibrium density, $v_t$ is the thermal speed, and $m$ stands for mass of the constituent particle). As a result the degeneracy pressure is larger than the thermal pressure so the Fermi energy of the particles exceeds the thermal energy. Hence, quantum signatures such as the quantum tunneling effect (via Bohm potential), quantum degeneracy pressure, exchange-correlation, and spin effect cannot be ignored in describing the particle dynamics and collective modes in such systems [2,10].

The classical magnetohydrodynamic (MHD) theory is extended to magnetized quantum plasmas via incorporation in the infinite conductivity limit developing quantum magneto-hydrodynamic (QMHD) model [10]. The introduction of spin effects in the QMHD model was proposed by Marklund and Brodin [11], where one fluid QMHD equation with electron spin-1/2 effect was derived with the help of the Pauli equation of an individual particle and also applied to dense plasma systems. Some of the works to mention here are those on linear waves [12,13], nonlinear waves [14,15], low frequency waves [16,17], solitons [18], shock waves [19–21], and references therein. Furthermore, the kinetic formalism for spin quantum plasmas has also been developed, taking the dynamics of the spin introduced via extended phase space [22,23]. Recent studies reveal that spin effects lead to the existence of new modes such as spin waves in quantum plasmas [24,25]. The linear and nonlinear two dimensional magnetosonic waves were investigated via a QMHD model featuring Bohm potential and spin effects via a magnetization term [26]. The spin-electron-acoustic waves and Langmuir waves were reported in a spin polarized plasma [27]. The effect of electron spin on kinetic Alfvén waves were studied in the presence of a static magnetic field where the wave frequency decreases due to the spin contribution [28]. Separate evolution of spin-up and spin-down electrons of different concentration introduces spin electrostatic waves which depend on the spin polarization density ratio in magnetized plasma [29].

In our present work we aim to study magnetosonic shock waves in spin polarized plasma via Bohm potential, spin polarization, and dissipative effects. We consider the separate evolution of spin-up and spin-down electrons to derive the Korteweg–de Vries–Burgers (KdVB) equation which leads to spin magnetosonic shock waves in spin-1/2 quantum plasmas.

 

The organization of the work is as follows: We present the developed model equations for the ion-scale electromagnetic excitations, propagating perpendicular to the external magnetic field, in Sec. II. The linear analysis is carried out in Sec. III. The analytical and numerical details of the small amplitude magnetosonic shock waves in spin polarized plasma are given in Sec. IV. Finally, we summarize our results in the concluding Sec. V.

## II. MODEL EQUATIONS

We consider quantum electron-ion magnetoplasma having classical ions and spin-up and spin-down nonrelativistic degenerate electrons. In the Cartesian coordinate system, the external magnetic field and spin magnetization are assumed to be along the $z$ direction and can be expressed as $\overrightarrow{B} = B(x,t)\hat{z}$ and $\overrightarrow{M} = M(x,t)\hat{z}$, respectively, where $\hat{z}$ is the unit vector along the $z$ coordinate. The one fluid QMHD model is considered in the framework of low frequency perturbations; therefore, we neglect the electron inertia and displacement current. The ion dynamical equations are given by [11,30]

$$m_i \frac{d\mathbf{v}_i}{dt} = e\mathbf{E} + e(\mathbf{v}_i \times \mathbf{B}) + \frac{\mathbf{R}_i}{n_i}, \tag{1}$$

$$\frac{\partial n_i}{\partial t} + \nabla \cdot (n_i \mathbf{v}_i) = 0. \tag{2}$$

The momentum equation for inertialess spin-up and spin-down electrons can be expressed as

$$0 = -n_{e\uparrow} e(\mathbf{E} + \mathbf{v}_{e\uparrow} \times \mathbf{B}) - \nabla P_{e\uparrow} + \mathbf{F}_{Q\uparrow} + \mathbf{R}_{e\uparrow}, \tag{3}$$

$$0 = -n_{e\downarrow} e(\mathbf{E} + \mathbf{v}_{e\downarrow} \times \mathbf{B}) - \nabla P_{e\downarrow} + \mathbf{F}_{Q\downarrow} + \mathbf{R}_{e\downarrow}, \tag{4}$$

and their continuity equations are

$$\frac{\partial n_{e\uparrow}}{\partial t} + \nabla \cdot (n_{e\uparrow} \mathbf{v}_{e\uparrow}) = 0, \tag{5}$$

$$\frac{\partial n_{e\downarrow}}{\partial t} + \nabla \cdot (n_{e\downarrow} \mathbf{v}_{e\downarrow}) = 0. \tag{6}$$

The spin vector ($\mathbf{S}$) appears during Marklund's decomposition of the wave function of the Pauli equation which is caused by the $\mathbf{S} \cdot \mathbf{B}$ interaction of the spin of each single particle. The space variation in spin modifies the spin magnetization and introduces a new spin pressure, also called the magnetic pressure. For the propagation of spin magnetosonic waves the spin evolution equation along with the above equations is given by

$$\frac{d\mathbf{S}}{dt} = \frac{2\mu_B}{\hbar}(\mathbf{S} \times \mathbf{B}). \tag{7}$$

The external magnetic field $\mathbf{B}$ is along the $z$ axis perpendicular to the wave propagation vector $k = k\hat{x}$, and $|\mu_B| = e\hbar/2m_e$ is the Bohr magneton. Here the spin of the electrons is chosen as a constant field and aligned antiparallel to the background magnetic field. The spin is not a dynamic variable; however, the spin pressure effect can vanish when the spin pressure is completely aligned, whereas the spin magnetization force effect cannot vanish in the momentum equation. Therefore, the spin term only appears in the usual spin magnetization force in the electron momentum equation. The spin flip can be produced when the temporal variations of the magnetic field are faster than the inverse electron cyclotron frequency. It can also be produced by particle collisions but it can be observed from the Pauli Hamiltonian that the probability for this type is far less than unity. Therefore, we consider dynamics on a time scale shorter than the inverse spin interaction frequency, but longer than the inverse cyclotron frequency; as a result, the spin flip can be neglected. It should also be noted that the inverse spin interaction frequency is greater than the inverse collision frequency. In such case the spin evolution equation becomes $\mathbf{S} \times \mathbf{B} = 0$, and gives the solution $\mathbf{S}_{\uparrow\downarrow} = \mp\hbar/2\hat{\mathbf{B}}$, with the $+$ $(-)$ sign for spin-up (spin-down) state electrons. Hence, the physics associated with spin flips can also be neglected and the continuity equation is conserved. The magnetization due to spin population electrons is $\mathbf{M}_{\uparrow\downarrow} = -2\mu_B n_{e\uparrow\downarrow}\mathbf{S}_{\uparrow\downarrow}/\hbar = \pm\mu_B n_{e\uparrow\downarrow}\hat{\mathbf{B}}$, which can also be written as $\mathbf{M} = \mu_B \tanh(\frac{\mu_B B}{T_{Fe}})\hat{\mathbf{B}}$, where the difference in spin-up and spin-down state electrons is proportional to $\tanh(\varepsilon)$ which is the Brillouin function due to magnetization of spin-1/2 electron distribution at thermodynamic equilibrium, i.e., $n_{e\uparrow} - n_{e\downarrow} = \tanh(\varepsilon) \approx \varepsilon$ with $\varepsilon(=\frac{\mu_B B}{T_{Fe}})$ the Zeeman energy normalized by temperature [11,30–33].

In the above set of equations, $d/dt = \partial/\partial t + (\mathbf{v}_i \cdot \nabla)$ is the hydrodynamic derivative, $\mathbf{v}_{i(e)}[=v_{i(e)}(x,t)\hat{x}]$ is the ion (electron) velocity along the $x$ direction, and the resistive term in our model represented by $\mathbf{R}_e = \mathbf{R}_{e\uparrow} + \mathbf{R}_{e\downarrow} = -\mathbf{R}_i = en_i\eta\mathbf{J}_p$ [34], where $\mathbf{J}_p = \sum_s q_s n_s \mathbf{v}_s$ $(s = i, e_\uparrow, e_\downarrow)$ is the plasma current density and $\eta = m_e\nu_{ei}/n_{0e}e^2$ is the plasma resistivity with electron-ion collisional frequency $\nu_{ei}$, $n_{0e}$ and $m_e$ being the electron unperturbed density and mass, respectively. Considering the spin-1/2 plasma, one may include the spin polarization effect of the degenerate electron gas to the pressure [35,36] as $P_e = \{\vartheta_{3D}(3\pi^2)^{2/3}\hbar^2 n_e^{5/3}\}/(5m_e)$, where $\vartheta_{3D} = [(1+\kappa)^{5/3} + (1-\kappa)^{5/3}]/2$ is the coefficient of spin polarization of the electron gas and $\hbar$ is the Planck constant. However, for unpolarized electrons the equation of pressure can be written as $P_e = \{(3\pi^2)^{2/3}\hbar^2 n_e^{5/3}\}/(5m_e)$. The partial pressures caused by the evolution of each spin-up and spin-down electron are $P_{e\uparrow} = \{(6\pi^2)^{2/3}\hbar^2 n_{e\uparrow}^{5/3}\}/(5m_e)$ and $P_{e\downarrow} = \{(6\pi^2)^{2/3}\hbar^2 n_{e\downarrow}^{5/3}\}/(5m_e)$, respectively. The relation of the electron concentration with the coefficient of spin polarization is presented as $n_e = n_{e\uparrow} + n_{e\downarrow}$, where $n_{e\uparrow} = (1+\kappa)n_e/2$ and $n_{e\downarrow} = (1-\kappa)n_e/2$. The quantum force $\mathbf{F}_{Q\uparrow\downarrow}$ on electron [18] is given by

$$\mathbf{F}_{Q\uparrow\downarrow} = \frac{n_{e\uparrow\downarrow}\hbar^2}{2m_e}\nabla\left(\frac{\nabla^2\sqrt{n_{e\uparrow\downarrow}}}{\sqrt{n_{e\uparrow\downarrow}}}\right) \pm \mu_B n_{e\uparrow\downarrow}\nabla B, \tag{8}$$

where the first term represents the quantum Bohm potential, whereas the second term represents the magnetization energy due to the spin-1/2 effect. Furthermore, $T_{Fe} = (3\pi^2 n_{0e})^{2/3}\hbar^2/(2m_e k_B)$ is the electron Fermi temperature measured in units of energy with Boltzmann constant $k_B$.

The Maxwell equations, i.e., Ampere's law in a magnetized medium, can take the form

$$\nabla \times \mathbf{B} = \mu_0(\mathbf{J}_p + \mathbf{J}_m), \tag{9}$$

$$\mathbf{J}_p = en_i\mathbf{v}_i - en_{e\uparrow}\mathbf{v}_{e\uparrow} - en_{e\downarrow}\mathbf{v}_{e\downarrow}, \tag{10}$$

where $\mathbf{J}_m = \nabla \times \mathbf{M}$ is the magnetization current density of electrons. The displacement current in Eq. (8) is neglected because of the low value compared to $J = J_p + J_m$ in a conducting medium (plasma). Faraday's law takes the form

$$\nabla \times \mathbf{E} = -\frac{\partial \mathbf{B}}{\partial t}, \tag{11}$$

and

$$\begin{aligned} \nabla \cdot \mathbf{B} &= 0, \\ \nabla \cdot \mathbf{E} &= 4\pi(en_i - en_{e\uparrow} - en_{e\downarrow}). \end{aligned} \tag{12}$$

The quasineutrality condition is assumed: $n_i \approx n_{e\uparrow} + n_{e\downarrow}$. It is important to mention here that we have neglected the ion cyclotron frequency, i.e., the ion gyrofrequency $\Omega_i$ under $\Omega_i \gg \omega$. The above set of one fluid QMHD momentum equations for ion, spin-up, and spin-down electrons with the help of Eqs. (9) may be written in normalized form as [21,37,38]

$$\begin{aligned} &n_i\left[\frac{\partial \mathbf{v}_i}{\partial t} + (\mathbf{v}_i \cdot \nabla)\mathbf{v}_i\right] \\ &= (\nabla \times \boldsymbol{B}) \times \mathbf{B} - \frac{2^{2/3}(\delta_\uparrow)^{5/3}\beta}{3} n_{e\uparrow}^{2/3} \nabla n_{e\uparrow} \\ &\quad - \frac{2^{2/3}(\delta_\downarrow)^{5/3}\beta}{3} n_{e\downarrow}^{2/3} \nabla n_{e\downarrow} + \frac{H_e^2 \delta_\uparrow}{2} n_{e\uparrow} \nabla\left(\frac{\nabla^2 \sqrt{n_{e\uparrow}}}{\sqrt{n_{e\uparrow}}}\right) \\ &\quad + \frac{H_e^2 \delta_\downarrow}{2} n_{e\downarrow} \nabla\left(\frac{\nabla^2 \sqrt{n_{e\downarrow}}}{\sqrt{n_{e\downarrow}}}\right) - (\nabla \times \mathbf{M}) \times \mathbf{B} + \varepsilon_0^2 \beta B \nabla B. \end{aligned} \tag{13}$$

The resistive term contributions in the above equation cancel to conserve the momentum of ions with electrons of spin-up and spin-down states separately, i.e., $-\mathbf{R}_i = \mathbf{R}_e = \mathbf{R}_{e\uparrow} + \mathbf{R}_{e\downarrow} = e(n_{e\uparrow} + n_{e\downarrow})\eta \mathbf{J}_p$. The normalized equation of continuity for the spin-up state electron by using Eqs. (1), (4), and (10) may be written as

$$\begin{aligned} &\frac{\partial n_{e\downarrow}}{\partial t} + \nabla \cdot \left[n_{e\downarrow}\left(\frac{\mathbf{B} \times (\mathbf{v}_i \times \mathbf{B})}{B^2}\right)\right] \\ &\quad + \nabla \cdot \left[n_{e\downarrow}\left(-\frac{\mathbf{B} \times (\nabla \times \mathbf{B}) \times \mathbf{B}}{n_i B^2} + \frac{\mathbf{B} \times (\nabla \times \mathbf{M}) \times \mathbf{B}}{n_i B^2}\right)\right] \\ &= 0. \end{aligned} \tag{14}$$

With the help of the ion momentum equation along with Eq. (10) the normalized magnetic induction equation can be obtained from Faraday's law [Eq. (11)] as

$$\frac{\partial \mathbf{B}}{\partial t} = \nabla \times (\mathbf{v}_i \times \mathbf{B}) - \gamma[\nabla \times (\nabla \times \mathbf{B})], \tag{15}$$

where we have neglected the anisotropic part of the pressure, which means that the ion gyrofrequency is much larger than the wave frequency ($\Omega_i \gg \omega$) and we also omitted the terms of order of $m_e/m_i$ compared with unity. Moreover, the Hall term and electron inertia are negligible in the standard QMHD model when the electron velocity is much higher than the ion velocity, whereas in the Hall-QMHD model the ion gyrofrequency may be comparable to the wave frequency ($\Omega_i \approx \omega$). The quantum force during these conditions is neglected in Ohm's law to obtain Eq. (15) [18,30,39]. Also Eq. (12) for spin magnetosonic waves may be written in normalized form as

$$n_i = \delta_\uparrow n_{e\uparrow} + \delta_\downarrow n_{e\downarrow}. \tag{16}$$

The number densities $n_s$ ($s = i, e_\uparrow, e_\downarrow$) are normalized by their respective equilibrium densities $n_{0s}$; other parameters are

$$r' = \frac{r\Omega_i}{V_A}, \quad \mathbf{v}_i' = \frac{\mathbf{v}_i}{V_A}, \quad \mathbf{B}' = \frac{\mathbf{B}}{B_0}, \quad t' = \Omega_i t, \quad n_s' = \frac{n_s}{n_{0s}},$$

where $\Omega_i = eB_0/m_i$ is the ion gyrofrequency, the Alfvén speed is $V_A = B_0/\sqrt{\mu_0 n_{0i} m_i}$, and plasma beta $\beta = \frac{c_{qs}^2}{V_A^2} = \frac{2\mu_0 n_{0i} \varepsilon_{Fe}}{B_0^2}$ measures the quantum statistical effects with $c_{qs} = \sqrt{\frac{2\varepsilon_{Fe}}{m_i}}$ the quantum ion sound speed, $n_{0i}$ the unperturbed density of ions, $\mu_0$ the permeability of free space with Fermi energy of a degenerate electron gas given as $\varepsilon_{Fe} = (3\pi^2 n_e)^{2/3}\hbar^2/(2m_e)$, and the dimensionless parameter $H_e = \hbar\Omega_i/(\sqrt{m_e m_i} V_A^2)$ appears due to collective electron tunneling through the Bohm potential. The normalized magnetization energy $\mathbf{M} = \mu_0 \mathbf{M}/B_0 = \varepsilon_0^2 \beta B \widehat{\mathbf{z}}$ with $\varepsilon_0 = \mu_B B_0/T_e$, and $\gamma = \eta\Omega_i/(\mu_0 V_A^2)$ is a dimensionless plasma dissipative parameter which shows that the diffusion term is inversely proportional to the background magnetic field $\mathbf{B}_0$. Furthermore, $\delta_\uparrow = n_{0e\uparrow}/n_{0i} = (1+\kappa)/2$, $\delta_\downarrow = n_{0e\downarrow}/n_{0i} = (1-\kappa)/2$, where the density polarization ratio $\kappa$ is given by

$$\kappa = \frac{n_{0e\uparrow} - n_{0e\downarrow}}{n_{0e\uparrow} + n_{0e\downarrow}}, \quad \kappa \in [0, 1]. \tag{17}$$

The unperturbed nonzero total concentration of the spin-up and spin-down electrons is $n_{e0} = n_{0e\uparrow} + n_{0e\downarrow}$, whereas the difference of the concentration of the spin-up and spin-down electrons $\nabla n_{e0} = n_{0e\uparrow} - n_{0e\downarrow}$ is caused by the external magnetic field $B_0$.

## III. DISPERSION RELATION OF MAGNETOSONIC WAVES

We exclusively derived a linear dispersion relation for magnetosonic waves with nonrelativistic degenerate spin-up and spin-down electrons as two independent species and classical ions, where we assumed small monochromatic perturbations of physical variables from the unperturbed state such as $n_{i1}$, $n_{e1\uparrow}$, $n_{e1\downarrow}$, $\mathbf{B}_1$, and $\mathbf{v}_{i1}$ present as $f = f_0 + \delta f$, whereas the linear excitations $\delta f$ are proportional to

$$\delta f = F_A e^{\iota(kx - \omega t)}, \tag{18}$$

where $F_A$ is the amplitude of the corresponding perturbation, $k$ is the perpendicular component of the wave vector, and $\omega$ is the wave frequency propagating along the $x$ direction. After linearizing Eqs. (13)–(16) and making use of formula (18) we obtained the dispersion relation as

$$\omega^3 + C_1\omega^2 + C_2\omega + C_3 = 0, \tag{19}$$

where $C_1$, $C_2$, and $C_3$ are respectively given by

$$\begin{aligned} C_1 &= i\gamma k^2, \\ C_2 &= k^2\left(2\varepsilon_0^2\beta - \frac{(1+\kappa)^{5/3}\beta}{6} - \frac{(1-\kappa)^{5/3}\beta}{6} - \frac{H_e^2 k^2}{4} - 1\right), \\ C_3 &= -i\gamma k^4\left(\frac{(1+\kappa)^{5/3}\beta}{6} + \frac{(1-\kappa)^{5/3}\beta}{6} + \frac{H_e^2 k^2}{4}\right). \end{aligned} \tag{20}$$

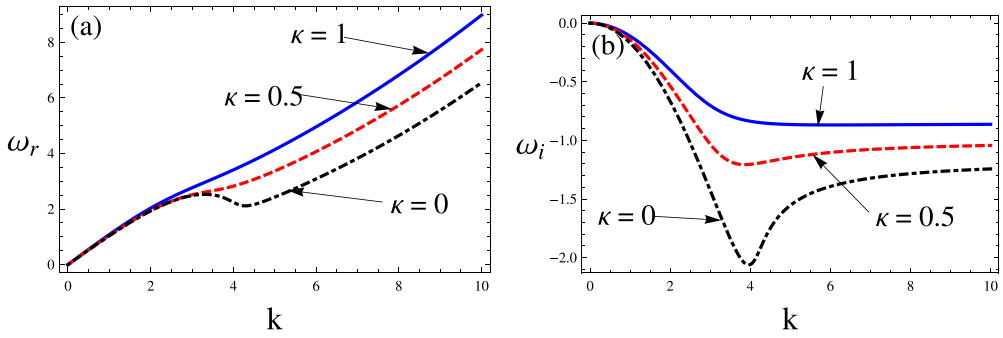


FIG. 1. (a) Real part of the dispersion relation $\omega_r$ against $k$ for different values of spin polarization ratio $\kappa$. (b) Imaginary part of the dispersion relation $\omega_i$ against $k$ for different values of $\kappa$, where $H_e = 0.1$, $\beta = 0.5$, $\epsilon_0 = 0.2$, and $\gamma = 0.4$.

The dispersion relation given in Eq. (19) is a third order equation describing low frequency $\omega$ for a spin magnetosonic wave having spin-up and spin-down electrons as two independent species. The spin polarization effects appear through $\kappa$ given by Eq. (17) such that $\kappa = 0$ means that half of the electrons are spin-up while half are spin-down. Furthermore, $\kappa = 1$ represents that the total electrons are either spin-up or spin-down, which is the usual electron ion quantum plasma situation.

Here we have plotted the real ($\omega_r$) and imaginary ($\omega_i$) part of the dispersion relation [Eq. (19)] against $k$ (the wave vector) for the spin polarization effect via $\kappa$ as shown in Fig. 1. One can see that the phase velocity of the magnetosonic waves is smaller in spin polarized plasma ($\kappa = 0$) compared to the usual electron-ion case configured via $\kappa = 1$. On the other hand, the induction of a spin polarized situation dampens the wave mode more slowly as shown in Fig. 1(b), and a high value can be noted at $k \approx 4$ and then the wave is damped more strongly for higher values of wave number.

Here we have reduced our dispersion relation based on Eq. (19) for previously derived results in the literature, for instance, $\kappa = 1$ in the above dispersion relation can be reduced to the dispersion relation in Ref. [21] in the presence of a diffusion term; similarly in the absence of a diffusion term one may obtain the usual dispersion relation of the magnetosonic waves as given in Ref. [38].

The numerical solution of the real and imaginary parts of the magnetosonic waves are plotted against $k$ for different values of plasma parameters such as diffusion ($\gamma$), quantum diffraction ($H_e$), Zeeman energy ($\varepsilon_0$), and plasma beta ($\beta$) as presented in Fig. 2. Increasing the dimensionless diffusion coefficient ($\gamma$) makes the real and imaginary parts of the dispersion relation decrease as shown in Figs. 2(a) and 2(b), respectively. It is important to mention that the effect of diffusion is greater in the longer $k$ regime on the real root of Eq. (19), whereas the imaginary root ($\omega_i$) is more sensitive to $\gamma$ against $k$ for the entire range. In Figs. 2(c) and 2(d), we have checked the effect of density correlation via $H_e$ on the real ($\omega_r$) and imaginary ($\omega_i$) frequency of the magnetosonic waves in spin polarized plasma. It is obvious that increasing the value of $H_e$ gives more dispersion in the medium. The upshot of wave frequency with $H_e$ is negligible in the longer wavelength regime (shorter $k$) on both the roots. It should be mentioned that for small values of $H_e$ the $\omega_i$ is damping while for higher values of $H_e$ it is growing more positive, as is clear from Fig. 2(d). In Figs. 2(e) and 2(f), we have shown the effect of changing the Zeeman energy via $\varepsilon_0$ on the wave modes based on Eq. (19) while the plasma beta ($\beta$) effect is depicted in Figs. 2(g) and 2(h) on the respective wave modes. One can see that the real frequency of the magnetosonic waves does not change significantly with both $\varepsilon_0$ and $\beta$; however, the damping rate is sensitive to both changing the Zeeman energy and also on plasma beta, as shown in Figs. 2(f) and 2(h).

## IV. SMALL AMPLITUDE SHOCKS

We consider the nonlinear wave propagation of magnetosonic shock structures in a planar geometry with separated spin-up and spin-down electrons and nondegenerate ions. Employing the standard reductive perturbation technique, the space and time variables can be stretched as [40]

$$\xi = \epsilon^{1/2}(x - V_0 t), \quad \tau = \epsilon^{3/2} t, \tag{21}$$

where the small parameter $\epsilon$ measures the strength of nonlinearity. The wave phase velocity $V_0$ is normalized by the Alfvén speed $V_A$ which will be determined from the first order expansion. We expand the dynamical variables in terms of $\epsilon$ as

$$\begin{aligned} n_s &= 1 + \epsilon n_{s1} + \epsilon^2 n_{s2} + \cdots, \\ B &= 1 + \epsilon B_1 + \epsilon^2 B_2 + \cdots, \\ v_i &= \epsilon v_{i1} + \epsilon^2 v_{i1} + \epsilon^3 v_{i2} + \cdots. \end{aligned} \tag{22}$$

It should be mentioned here that along with the above expansion the resistive term $\gamma = \epsilon^{1/2}\gamma_0$ [41] will make the perturbation evolution equation consistent, where $\gamma_0 \simeq 1$. The resistive term in the momentum equation is almost linearly proportional to the number density; therefore, we expanded $\gamma$ in the lower order of $\epsilon$ to see the dissipation of magnetosonic shock waves numerically. Such a small consideration of the damping term can be found in the literature and in many experimental situations [42,43]. If the $\gamma_0$ is a large value one can use the same consideration as used in Ref. [42], where the only difference is that for large values, i.e., $\gamma = \epsilon\gamma_0$, a sharp rising shock front has been observed as compared to oscillatory and monotonic shock waves (for $\gamma = \epsilon^{1/2}\gamma_0$). Using the stretching [Eq. (21)] and expansions [Eq. (22)] in Eqs. (2) and (13)–(15) and collecting the lowest order terms in $\epsilon$, we get the wave phase velocity mentioned in Eq. (21) in the presence of spin-up and spin-down degenerate electrons,

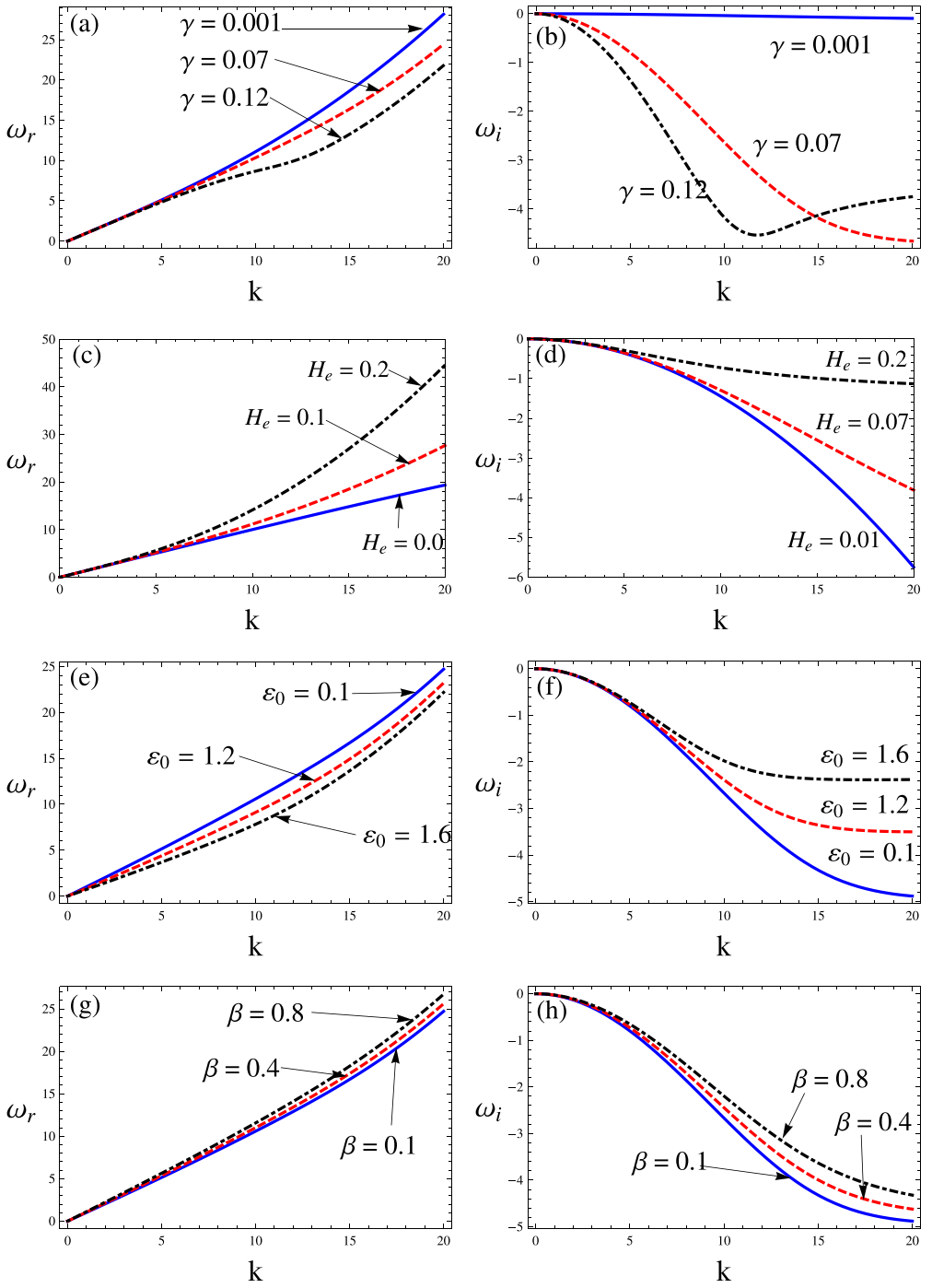


FIG. 2. Real and imaginary parts of the plasma normalized angular frequency of dispersion relation (19) against $k$ for different values of dimensionless plasma variables such as diffusion ($\gamma$), quantum diffraction ($H_e$), plasma beta ($\beta$), and Zeeman energy ($\epsilon_0$). (a), (b) Plots for different values of $\gamma$ for $H_e = 0.1$, $\beta = 0.1$, and $\epsilon_0 = 0.5$; (c), (d) plots for different values of $H_e$ where $\beta = 0.1$, $\varepsilon_0 = 0.2$, and $\gamma = 0.03$; (e), (f) plots for different values of $\varepsilon_0$ where $H_e = 0.1$, $\beta = 0.1$, and $\gamma = 0.07$; and (g), (h) plots for different values of $\beta$ where $H_e = 0.1$, $\varepsilon_0 = 0.1$, and $\gamma = 0.07$.

given as

$$V_0 = \left[1 + \frac{(1+\kappa)^{5/3}\beta}{6} + \frac{(1-\kappa)^{5/3}\beta}{6} - 2\varepsilon_0^2\beta\right]^{1/2}. \quad (23)$$

Equation (23) exclusively shows that phase velocity depends on the spin polarization index $\kappa$, the plasma beta $\beta$, and Zeeman energy $\varepsilon_0$ and is independent of quantum diffraction $H_e$ and resistivity $\gamma$. The effects of spin state of the electron gas on phase velocity are shown in Fig. 3, which shows that for low values of spin polarization (meaning spin-up and spin-down electrons remain independent species) the phase velocity has smaller values and then approaches a maximum value for $\kappa \to 1$ (usual electron ion quantum plasma).

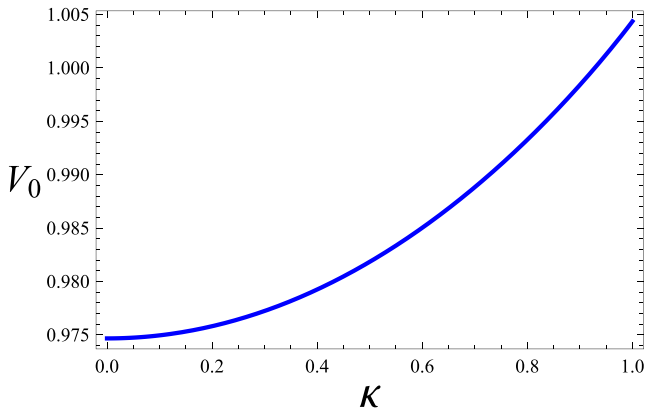


FIG. 3. Phase velocity ($V_0$) defined by Eq. (23) against spin polarization density ratio $\kappa$ for $\beta = 0.3$, $\epsilon_0 = 0.5$.

For the next higher order terms in $\epsilon$ with the help of first order quantities we obtain the following KdVB equation:

$$\frac{\partial B_1}{\partial t} + QB_1\frac{\partial B_1}{\partial \zeta} + R\frac{\partial^3 B_1}{\partial \zeta^3} - D\frac{\partial^2 B_1}{\partial \zeta^2} = 0. \tag{24}$$

The coefficients of the KdVB equation (24) are the nonlinear $Q$, dispersion $R$, and dissipation $D$. Based on our plasma configuration, the coefficients acquire the following mathematical forms:

$$Q = \frac{1}{2V_0}\left[2V_0^2 + 1 + \frac{(1+\kappa)^{5/3}\beta}{9} + \frac{(1-\kappa)^{5/3}\beta}{9} - 4\varepsilon_0^2\beta\right], \tag{25}$$

$$R = -\frac{H_e^2}{8V_0}, \tag{26}$$

and

$$D = \frac{\gamma_0}{2V_0^2}\left[V_0^2 - \frac{(1+\kappa)^{5/3}\beta}{6} - \frac{(1-\kappa)^{5/3}\beta}{6}\right]. \tag{27}$$

In the absence of dissipation in the medium, i.e., setting $D \to 0$, one can obtain the well-known Korteweg–de Vries (KdV) equation from our Eq. (24) and a stationary soliton solution can be obtained for solitary pulses. On the other hand, modeling situations of negligible dispersion as compared to dissipation in the medium, i.e., $R \to 0$, reduces to the Burgers equation bearing a stationary shock profile. Here we proceed with an oscillatory shock wave solution based on Eq. (24). The magnetic diffusivity parameter $\gamma_0$ in the present model yields the formation of shock structures. For our reader it is important to mention that our results agree with Ref. [21] in the limit $\kappa = 1$ (usual electron ion quantum plasma). The coefficients of KdVB equation (24) can be cast to the one given in Ref. [21].

The stability of the shock waves is carried out here following the procedure of Refs. [44,45]. The stationary wave frame $\chi = \zeta - U_0\tau$ is used to transform Eq. (24), where $U_0$ is the constant velocity of the frame. The transformed equation is given below:

$$R\frac{d^3 B_1}{d\chi^3} = U_0\frac{dB_1}{d\chi} - QB_1\frac{dB_1}{d\chi} + D\frac{d^2 B_1}{d\chi^2}. \tag{28}$$

Integrating the above equation with respect to $\chi$ once and applying the boundary conditions $B_1 \to 1$ and $dB_1/d\chi \to 0$ as $\chi \to \pm\infty$ we get

$$\frac{d^2 B_1}{d\chi^2} = \frac{1}{R}\left[\frac{Q}{2} - U_0 + U_0 B_1 - \frac{Q}{2}B_1^2 + D\frac{dB_1}{d\chi}\right]. \tag{29}$$

The above second order differential equation can be expressed in terms of two separate first order equations:

$$\frac{dB_1}{d\chi} = Z,$$
$$\frac{dZ}{d\chi} = \frac{1}{R}\left[\frac{Q}{2} - U_0 + U_0 B_1 - \frac{Q}{2}B_1^2 + DZ\right]. \tag{30}$$

The above pair of equations has two fixed points, i.e., $(B_1 = 1, Z = 0)$ and $(B_1 = 2U_0/Q - 1, Z = 0)$, showing the equilibrium downstream and upstream states, respectively. The upstream singular point is a stable focus or stable node and the downstream $(1, 0)$ is always a saddle point. The stable focus point gives the oscillatory nature of shocks, whereas the stable node results in the monotonic nature of the solution. For numerical simulation of shock wave characteristics, one may solve Eq. (30) numerically with the help of MATHEMATICA software by taking the initial values $B_1(\chi = 0) = 1$, $Z(\chi = 0) = -10^{-5}$. The initial values can vary between the stable focus and saddle point, i.e., $B_1(\chi = 0) = 1 \to (2U_0/Q - 1)$, whereas $Z(\chi = 0) \approx 0$.

To investigate the oscillatory or shock wave behavior we study numerically the dynamics of magnetosonic shock waves bearing a spin polarization effect via system (30) for different plasma configurations. Our results show that for certain values of plasma parameters the dispersion effect dominates over the dissipative term so that oscillatory shock profiles are formed; otherwise, the behavior is monotonic. Figure 4 shows how the plasma beta ($\beta$) affects the shock structure: as the value of $\beta$ gets larger, the oscillatory shock amplitude decreases and some oscillations still exist for $\kappa = 1$ (spin quantum plasma having electrons of either up or down polarity relative to the external field), while the monotonic behavior is obtained for larger values of $\beta$ for the case of a spin polarized situation configured via $\kappa = 0$ (meaning half of the electrons are spin-up and half are spin-down). It means that the waves dissipate more quickly in degenerate spin polarized quantum plasma than in usual ion electron plasma. Figure 5 depicts the behavior of normalized Zeeman energy on the magnetosonic shock waves. One can see that for higher values of $\varepsilon_0$ the oscillatory shocks convert to a monotonic nature. Interestingly more oscillations with large amplitude can be seen for usual electron ion quantum degenerate plasma ($\kappa = 1$) than for the spin polarized situation, i.e., $\kappa = 0$. The quantum diffraction appears due to the density correlation strongly affecting the shock structure as shown in Fig. 6. For small values of $H_e$ the waves remain monotonic in both spin configurations, i.e., $\kappa = 0$ and 1, while for higher values of $H_e$ the shock converts to oscillatory behavior. Small values of $H_e$ correspond to small dispersion of shocks which results in a monotonic nature as the medium yields more dissipative effects than the dispersion.

Furthermore, the wave amplitude is larger for the $\kappa = 1$ case and shows more oscillation than the $\kappa = 0$ layout.

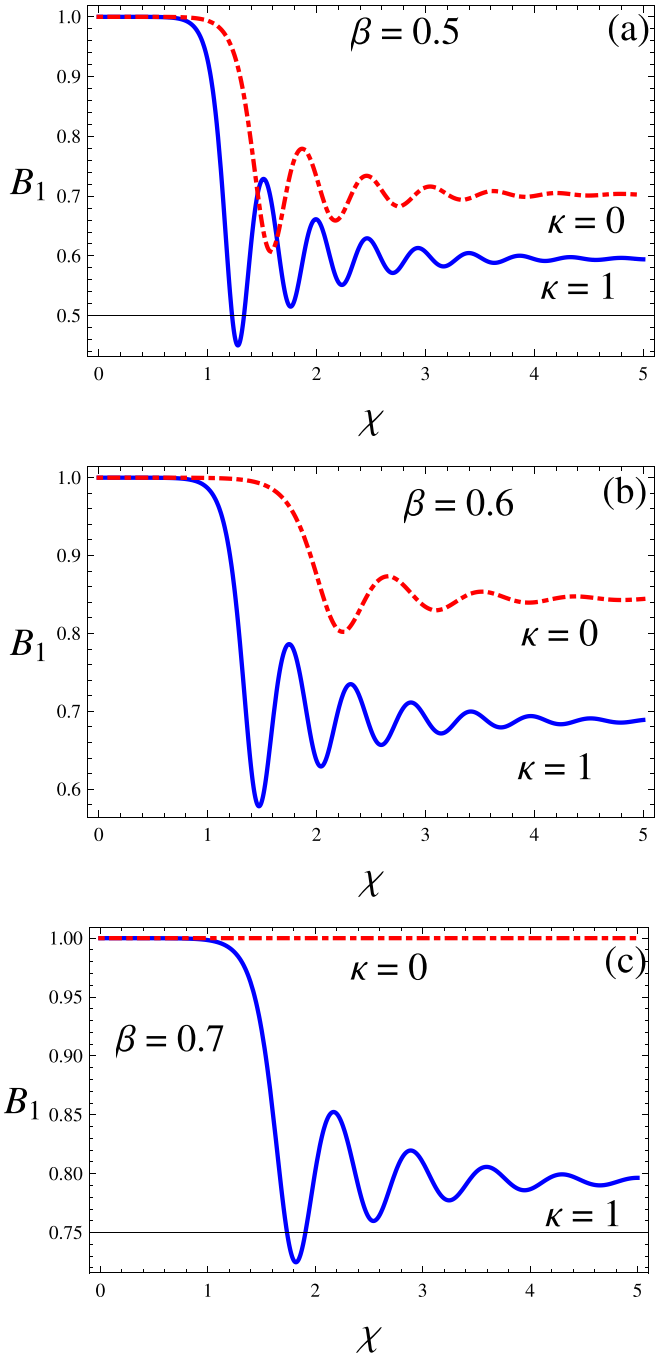


FIG. 4. Shock wave represented by Eq. (30) for different values of $\beta$ where $H_e = 0.1$, $\varepsilon_0 = 0.6$, $\gamma_0 = 0.01$, $U_0 = 0.95$.

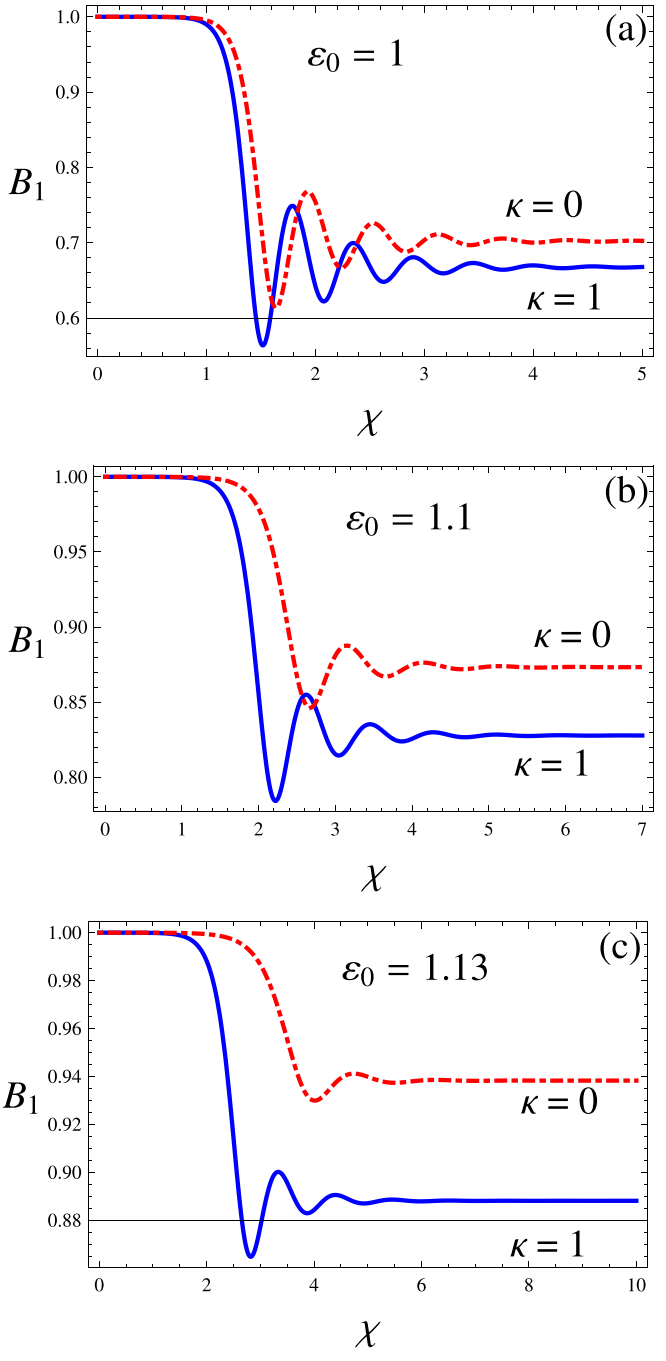


FIG. 5. Shock profile represented by Eq. (30) for different values of spin magnetic energy $\varepsilon_0$, where $H_e = 0.1$, $\beta = 0.15$, $\gamma_0 = 0.01$, $U_0 = 0.95$.

Figure 7 shows the effects of the diffusion term on shock structures; one can see that as the resistivity increases the dissipation dominates over the dispersion and the shock wave emits a monotonic profile with increasing amplitude once $\gamma_0$ crosses the critical value. Again the damping is found less prominent in the usual electron ion plasma ($\kappa = 1$) compared to the spin polarized plasma for which half of the electrons are spin-up and half are spin-down, modeled via $\kappa = 0$. Phase portraits of system (30) corresponding to Figs. 4–7 are presented in Figs. 8–11. For low values of plasma parameters such as plasma beta ($\beta$), Zeeman energy ($\varepsilon_0$), and magnetic resistivity ($\gamma_0$) for both situations (i.e., $\kappa = 0, 1$), we observed a series of oscillations where few of them correspond to solitary waves. As the values of the above mentioned plasma parameters increase, the phase-space trajectories show a closed orbit and tend to dissipate strongly; thereby the oscillatory nature reduces to a monotonic one. For low values of magnetic energy the number of aperiodic oscillations seems to be more as compared to those observed for higher values of $\varepsilon_0$ as evident from Fig. 9.

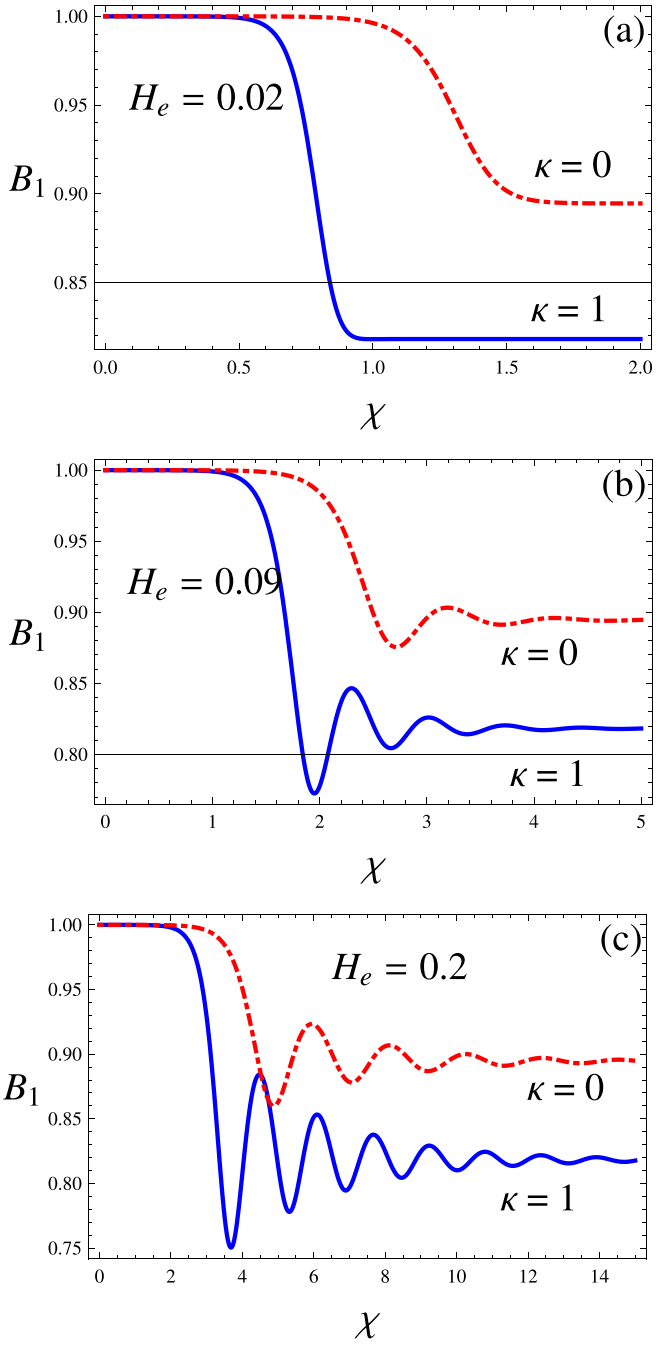


FIG. 6. Shock profile represented by Eq. (30) for different values of quantum diffraction ($H_e$) where $\varepsilon_0 = 0.88$, $\beta = 0.25$, $\gamma_0 = 0.01$, $U_0 = 0.95$.

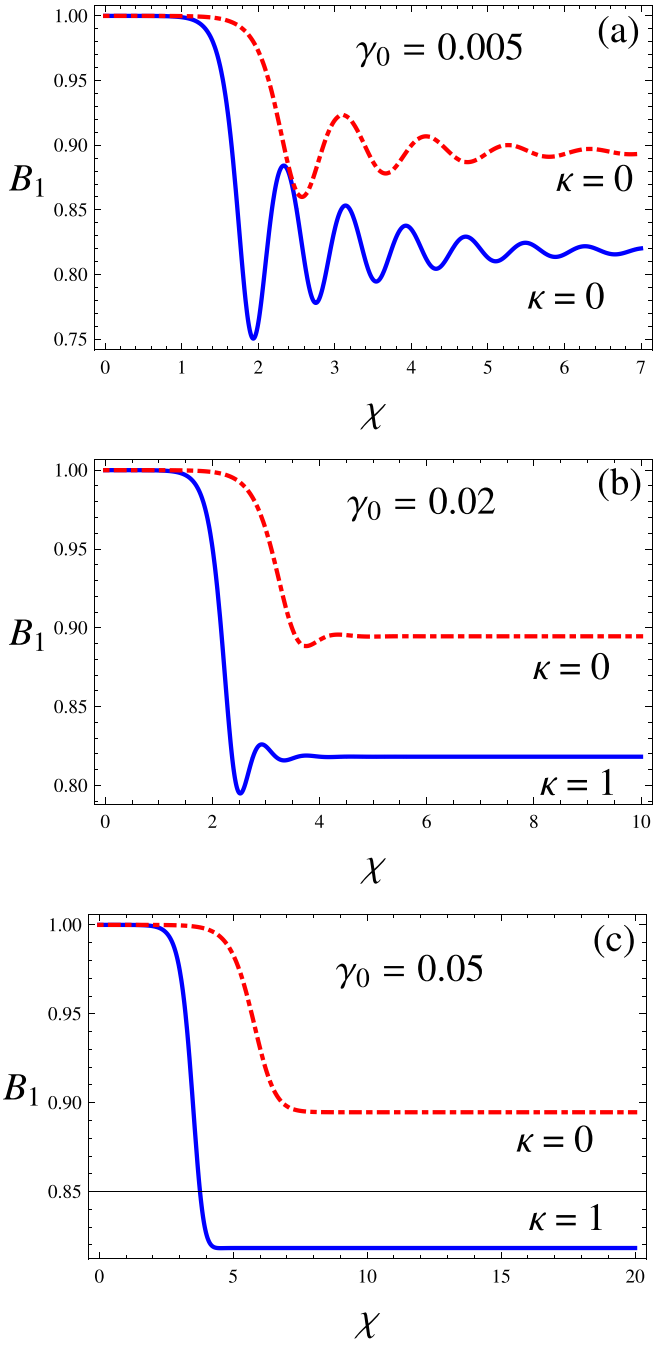


FIG. 7. Shock profile represented by Eq. (30) for different values of plasma diffusivity ($\gamma_0$) where $\varepsilon_0 = 0.88$, $H_e = 0.1$, $\beta = 0.25$, $U_0 = 0.95$.

Moreover, for $\kappa = 1$ the amplitudes of shock oscillations are larger and approach to a saddle point more slowly. It means that damping is more prominent in the spin polarized plasma medium than in the usual ion electron degenerate plasma. The phase portrait is influenced by the quantum Bohm potential as expressed in Fig. 10. It is observed that for low values of $H_e$ the shock waves are strongly damped and favor monotonic structures, whereas for higher $H_e$ the waves show an oscillatory behavior with larger amplitude. Furthermore, less dissipation and more oscillations are observed for $\kappa = 1$ than for the $\kappa = 0$ layout.

## V. CONCLUSIONS

We have investigated exclusively the linear and nonlinear magnetosonic shock waves bearing spin-up and spin-down electrons as two separate species. The effects of quantum dissipation, quantum diffraction $H_e$, plasma beta $\beta$, energy of the spin-up and spin-down electrons characterized by the spin pressure parameters via $\varepsilon_0$, magnetic diffusivity $\gamma_0$, and spin polarization $\kappa$ are traced out. The numerical data are chosen for dense astrophysical objects such as pulsar magnetospheres [46], where plasma densities are $n_0 = 10^{30}$–$10^{36}$ m$^{-3}$. For

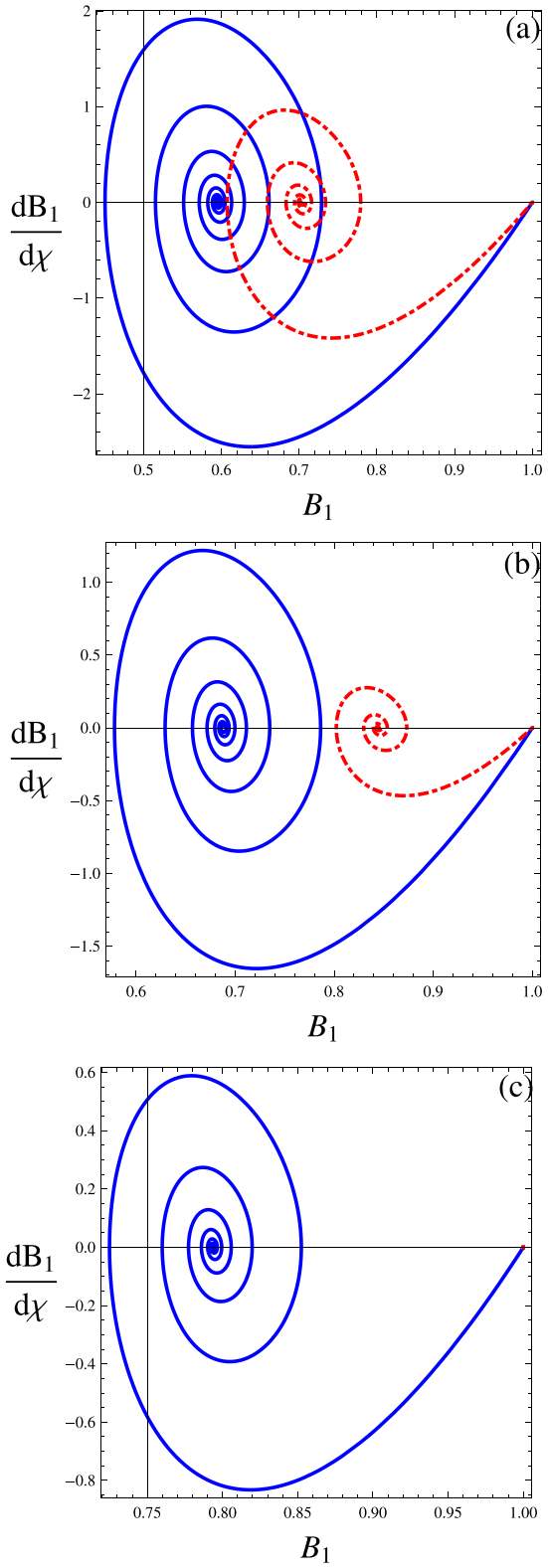


FIG. 8. The phase portraits corresponding to Fig. 4.

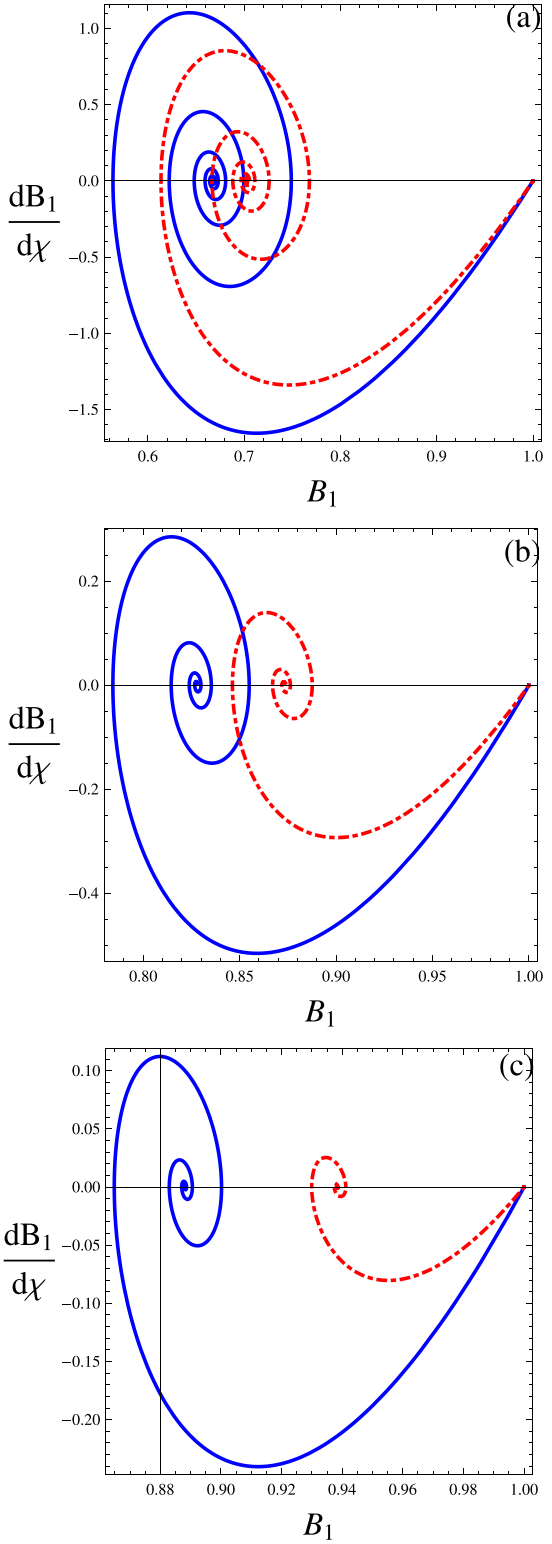


FIG. 9. The phase portraits corresponding to Fig. 5.

such types of system, $H_e \leqslant 1$, $\beta$ has some finite value $\leqslant 1$, $\varepsilon_0 \geqslant 1$, $\gamma_0 < 1$, and spin polarization $\kappa$ has values of zero and 1. We noticed that the shock waves were produced due to the balance of the nonlinear and dissipation coefficients. When the nonlinearity is balanced by the combined effects of dispersion, which depends on $H_e$ and dissipation, an oscillatory or monotonic shock structures are produced in plasma. On the other hand, when the dissipation is small a few oscillations are very close to a soliton, while large dissipation is responsible for the formation of an aperiodic and monotonic profile. At the first step, we numerically solve the linear

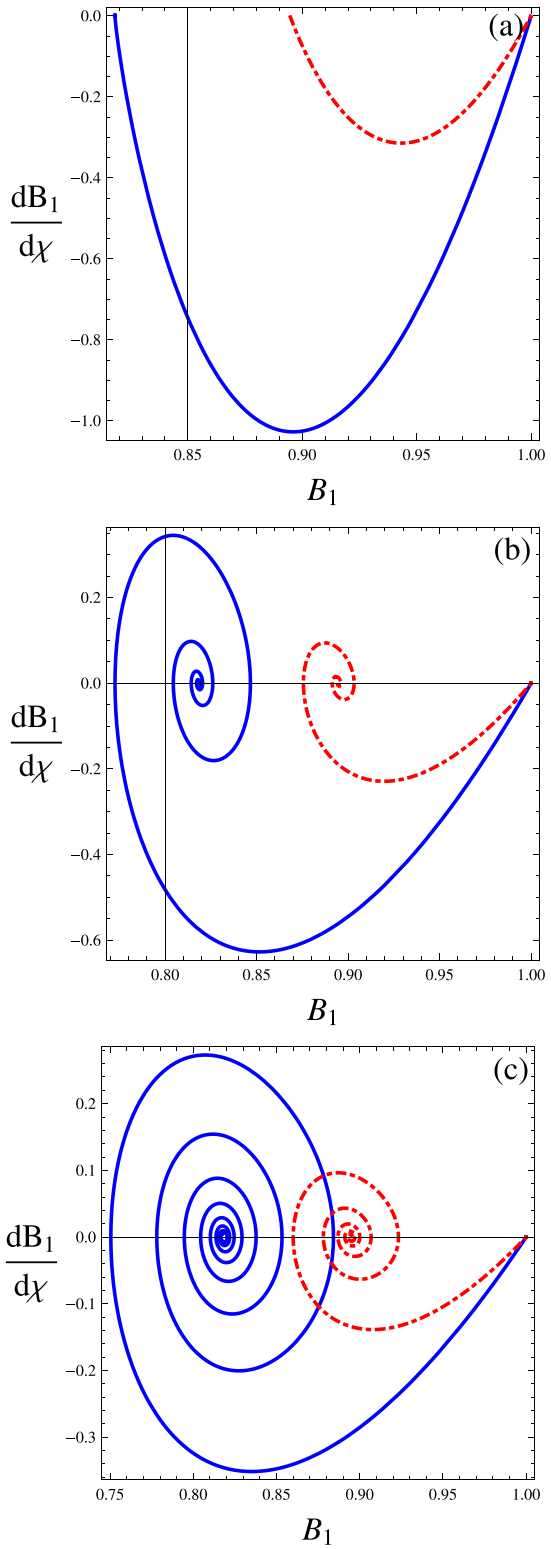


FIG. 10. The phase portraits corresponding to Fig. 6.

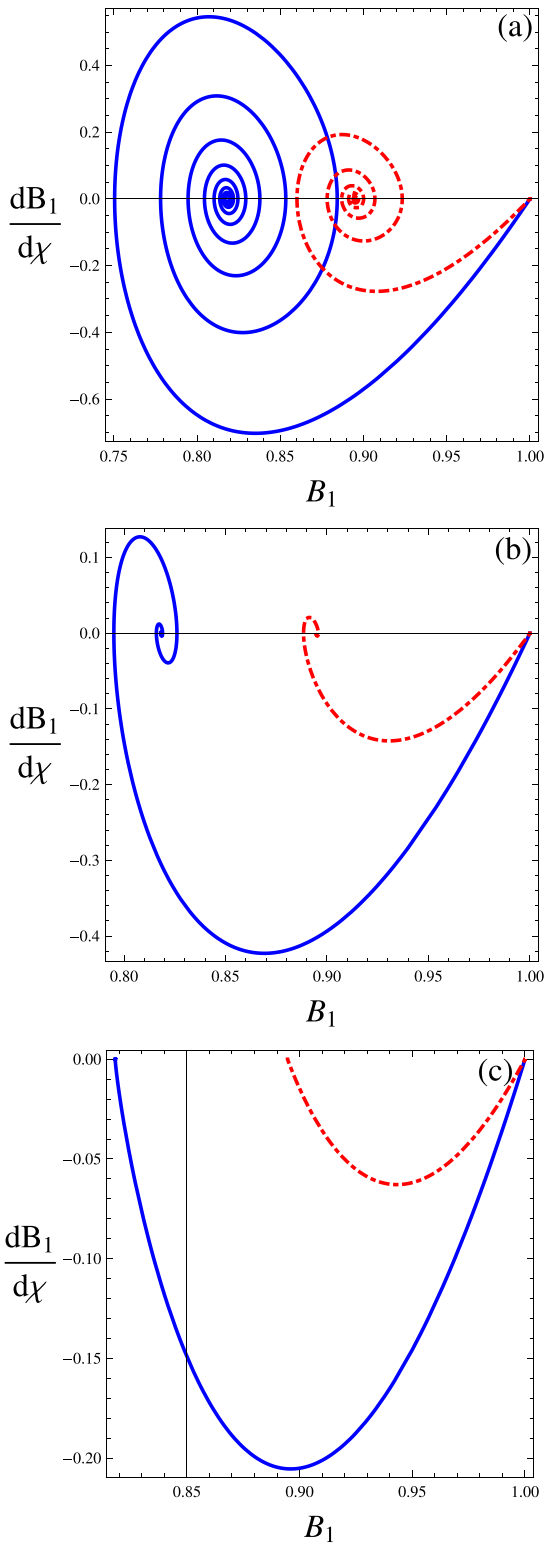


FIG. 11. The phase portraits corresponding to Fig. 7.

dispersion relation [Eq. (19)] of magnetosonic waves and study the effects of different plasma parameters. The presence of the magnetic diffusive term is responsible for the complex plasma wave frequency $\omega = \omega_r + \iota\omega_i$, so diffusion is the cause of wave damping in plasma. The magnitude of $\omega_r$ increases and dissipation $\omega_i$ is large for $\kappa = 0$ and vice versa for $\kappa = 1$. Similarly $\omega_r$ decreases and damping increases with the increase of $\varepsilon_0$ and $\gamma_0$, whereas the amplitude of $\omega_r$ increases and damping decreases with higher values of $\beta$ and $H_e$. At the second stage, the small amplitude analysis results in the KdVB equation [Eq. (24)] in the framework of the reductive perturbation technique. The result shows the influence of spin

polarization ($\kappa$) on phase velocity, i.e., the phase velocity of the waves is a minimum with spin-up and spin-down electrons and a large value for usual electron ion plasma. The numerical solution of the KdVB equation [Eq. (30)] leads to oscillatory and monotonic shock waves depending upon the plasma variable. For low values of $\beta$, $\varepsilon_0$, and $\gamma_0$, system (30) results in an oscillatory shock profile while for higher values one can get the monotonic structures. On the other hand, for smaller values of quantum diffraction parameter ($H_e$) the dissipation is large and produces monotonic shocks and oscillatory shock structures with small damping for higher values of $H_e$.

Finally the phase portrait of the corresponding monotonic and oscillatory magnetosonic shock waves is presented. The results should be useful for understanding the linear and small amplitude nonlinear propagation of oscillatory and monotonic shock waves that can be produced in some dense astrophysical plasma systems such as magnetic pulsars, magnetic white dwarfs, and neutron stars, where degenerate spin-up and spin-down electrons with dissipative effects can be found.

## ACKNOWLEDGMENTS

The authors acknowledge the anonymous referees for useful suggestions that led to the improvement of the paper. One of the authors (M.A.) warmly acknowledges the financial support of the Higher Education Commission of Pakistan under Project No. 9034.

[1] F. Haas, *Quantum Plasma: A Hydrodynamic Approach* (Springer-Verlag, New York, 2011).
[2] G. Manfredi, Fields Inst. Commun. **46**, 263 (2005).
[3] S. L. Shapiro and S. A. Teukolsky, *Black Holes, White Dwarfs, and Neutron Stars: The Physics of Compact Objects* (Wiley-VCH, Weinheim, 2004).
[4] T. D. Lee, Astrophys. J. **111**, 625 (1950).
[5] W. B. Hubbard, Astrophys. J. **146**, 858 (1966).
[6] M. Marklund and P. K. Shukla, Rev. Mod. Phys. **78**, 591 (2006).
[7] S. H. Glenzer, G. Gregori, R. W. Lee, F. J. Rogers, S. W. Pollaine, and O. L. Landen, Phys. Rev. Lett. **90**, 175002 (2003).
[8] A. Jungel, *Transport Equations for Semiconductor Devices* (Springer, Berlin, 2009).
[9] R. Bonifacio, C. Pellegrini, and L. Narducci, Opt. Commun. **50**, 373 (1984).
[10] F. Haas, Phys. Plasmas **12**, 062117 (2005).
[11] M. Marklund and G. Brodin, Phys. Rev. Lett. **98**, 025001 (2007).
[12] G. Brodin and M. Marklund, Phys. Rev. E **76**, 055403(R) (2007).
[13] P. K. Shukla, Phys. Lett. A **369**, 312 (2007).
[14] S. Ali, W. M. Moslem, P. K. Shukla, and I. Kourakis, Phys. Lett. A **366**, 606 (2007).
[15] P. K. Shukla, S. Ali, L. Stenflo, and M. Marklund, Phys. Plasmas **13**, 112111 (2006).
[16] F. Haas, L. G. Garcia, J. Goedert, and G. Manfredi, Phys. Plasmas **10**, 3858 (2003).
[17] H. Saleem, Ali Ahmad, and S. A. Khan, Phys. Plasmas **15**, 014503 (2008).
[18] M. Marklund, B. Eliasson, and P. K. Shukla, Phys. Rev. E **76**, 067401 (2007).
[19] A. P. Misra and N. K. Ghosh, Phys. Lett. A **372**, 6412 (2008).
[20] W. Masood, S. Karim, and H. A. Shah, Phys. Scr. **82**, 045503 (2010).
[21] B. Sahu, S. Choudhury, and A. Sinha, Phys. Plasmas **22**, 022304 (2015).
[22] G. Brodin, M. Marklund, J. Zamanian, A. Ericsson, and P. L. Mana, Phys. Rev. Lett. **101**, 245002 (2008).
[23] J. Lundin and G. Brodin, Phys. Rev. E **82**, 056407 (2010).
[24] D. V. Vagin, N. E. Kim, P. A. Polyakov, and A. E. Rusakov, Izv. Ross. Akad. Nauk, Energ. **70**, 443 (2006).
[25] P. A. Andreev and L. S. Kuz'menkov, Moscow Univ. Phys. Bull. **62**, 271 (2007).
[26] A. Mushtaq and S. V. Vladimirov, Phys. Plasmas **17**, 102310 (2010).
[27] P. A. Andreev, Phys. Rev. E **91**, 033111 (2015).
[28] A. Hussain, Z. Iqbal, G. Brodin, and G. Murtaza, Phys. Lett. A **377**, 2131 (2013).
[29] R. Ahmad, N. Gul, M. Adnan, and F. Y. Khattak, Phys. Plasmas **23**, 112112 (2016).
[30] G. Brodin and M. Marklund, New J. Phys. **9**, 277 (2007).
[31] G. Brodin, M. Marklund, and G. Manfredi, Phys. Rev. Lett. **100**, 175001 (2008).
[32] G. Brodin, A. P. Misra, and M. Marklund, Phys. Rev. Lett. **105**, 105004 (2010).
[33] J. Chen and D. H. E. Dubin, Phys. Fluids B **5**, 691 (1993).
[34] J. P. Goedbloed and S. Poedts, *Principles of Magnetohydrodynamics* (Cambridge University Press, Cambridge, 2004).
[35] L. S. Kuz'menkov, S. G. Maksimov, and V. V. Fedoseev, Theor. Math. Phys. **126**, 212 (2001).
[36] P. A. Andreev, Ann. Phys. **350**, 198 (2014).
[37] W. Masood and A. Mushtaq, Phys. Lett. A **372**, 4283 (2008).
[38] A. Mushtaq and S. V. Vladimirov, Eur. Phys. J. D **64**, 419 (2011).
[39] G. Brodin and L. Stenflo, Contrib. Plasma Phys. **30**, 413 (1990).
[40] H. Washimi and T. Taniuti, Phys. Rev. Lett. **17**, 996 (1966).
[41] M. Bartuccelli, P. Carbonaro, and V. Muto, Lett. Nuovo Cimento Soc. Ital. Fis. **42**, 279 (1985).
[42] Y. Nakamura and A. Sarma, Phys. Plasmas **8**, 3921 (2001).
[43] Y. Nakamura and H. Bailung, Phys. Rev. Lett. **83**, 1602 (1999).
[44] M. Belic, N. Petrovic, W. P. Zhong, R. H. Xie, and G. Chen, Phys. Rev. Lett. **101**, 123904 (2008).
[45] S. Ghosh, N. Chakrabarti, and P. K. Shukla, Phys. Plasmas **19**, 072123 (2012).
[46] A. K. Harding and D. Lai, Rep. Prog. Phys. **69**, 2631 (2006).